Acta Mechanica Slovaca **30 (1): 20 - 24,** March **2026**
https://doi.org/10.21496/ams.2026.004

Acta Mechanica Slovaca
ISSN 1335-2393
www.actamechanica.sk

Numerical Analysis of the Buildability of a 3D-Printed Cylindrical Concrete Wall: A VoxelPrint–Abaqus Approach

Erika Dubňanská [1,*], Martina Hančinová [1], Jakub Mlotek [2], Zdenko Bobovský [2], Martin Hagara [1], Róbert Huňady [1]

[1] Technical University of Košice, Faculty of Mechanical Engineering, Department of Applied Mechanics and Mechanical Engineering, Letná 1/9, 042 00 Košice, Slovak Republic
[2] VŠB - Technical University of Ostrava, Faculty of Mechanical Engineering, Department of Robotics, 17. listopadu 2172/15, 708 00 Ostrava-Poruba, Czech Republic

Abstract: Additive manufacturing (AM) of silicate-based materials has emerged as a significant research area, with adoption across construction, automotive and electrical engineering, as well as art and design. The rheology of fresh mixtures, along with process parameters (printing speed, layer height, bead width), strongly influences printability and buildability. In addition to experiments, numerical methods – particularly finite-element analysis – are increasingly used to predict the structural response and assess the stability of printed components. This study investigates the buildability of an extrusion-printed cylindrical concrete wall using a finite-element modelling (FEM) approach. A parametric model was created in VoxelPrint – a Grasshopper plug-in – and exported as an Abaqus input file (.inp) with the required model definitions (mesh, material properties, steps, boundary conditions, loads, and activation sets). To quantify discretization sensitivity, two voxel sizes were investigated – 8 mm and 4 mm. The model was analysed in Abaqus/Standard with stepwise element activation. Material behaviour was represented by a time-dependent material model based on the Mohr–Coulomb criterion, assuming a linear stress–strain response up to failure.

Keywords: numerical modelling; numerical simulation; 3D printing; silicate materials, concrete 3D printing; VoxelPrint, Abaqus

1. Introduction

Additive manufacturing, often referred to as 3D printing, has become one of the most important manufacturing technologies of the past decade. In this process, components are fabricated via layer-by-layer deposition of material along precisely defined toolpaths. For highly viscous paste-like silicate materials – such as ceramic clay, cementitious suspensions and concrete – the Direct Ink Writing (DIW) principle, classified under Material Extrusion (MEX), is generally regarded as the most suitable approach. The final quality and mechanical properties of the printed object are significantly influenced by the composition and rheology of the material mixture, as well as by printing parameters (layer height, layer width, printing speed, and extrusion speed). These factors govern printability – the ability of the fresh paste to be continuously extruded and deposited with dimensional accuracy [1–6].

In addition to printability, another key metric is buildability, defined as the capacity of the extruded filament and the growing layer-wise structure to resist deformation under self-weight and the loads from subsequent layers, thereby retaining shape during

*** Corresponding author:** Erika Dubňanská, ***E-mail address:*** *erika.dubnanska@tuke.sk*

printing. Operationally, it is quantified by the maximum buildable height (or number of layers) achievable without loss of structural stability (e.g. elastic buckling or plastic collapse). Insufficient buildability degrades dimensional accuracy and substantially increases the risk of collapse [7,8].

Beyond experimental testing, numerical mechanics is increasingly employed in this field. Finite-element analyses (FEA) of the printing process enable prediction of structural behaviour during deposition and identification of potential premature failure. At the filament scale, accurate representation of viscoplastic behaviour is crucial to capture time-dependent deformation, whereas at the structural scale, elastic–plastic modelling forms the basis for predicting global stability [9–11].

Wolfs et al. [9] investigated the mechanical behaviour of fresh concrete during 3D printing by combining numerical modelling with experimental testing. Finite-element analyses, based on a time-dependent Mohr–Coulomb failure criterion, revealed two dominant failure mechanisms: plastic collapse of the lower layers and elastic buckling of the upper layers. A non-contact optical measurement system was used to validate the simulated failure modes with those of the printed components.

Vantyghem et al. [12] presented a plug-in called VoxelPrint for the Grasshopper visual programming environment integrated into Rhinoceros 3D. The authors used VoxelPrint to create a 3D model discretized into voxels and analysed the influence of voxel size and the number of computational steps. Comparison of the maximum printable height and the failure mechanism with the study by Wolfs et al. [9] was in close agreement. Both approaches predicted a critical height of 460 mm, at which structural collapse occurred.

Buildability and failure mechanisms in extrusion-printed, paste-like structures were further investigated by Pierre et al. [13], Spangenberg et al. [14], and Ann et al. [15].

2. Numerical modelling and simulation

To assess the buildability of a cylindrical wall with a mean radius of 180 mm, a wall thickness of 16 mm, and a layer height of 8 mm, representing a structure produced by extrusion-based 3D printing, a parametric model was developed using the VoxelPrint plug-in. The voxelised model was then analysed in the commercial finite-element solver Abaqus/Standard.

VoxelPrint generates the Abaqus input file (.inp) through a sequence of interconnected components within the Grasshopper environment. The basic workflow comprises five components – two core (BrepToVoxel, VoxelToAbaqus) and three auxiliary (Material, PrintSettings, VoxelPreview). Each component requires specific input parameters to function. Figure 1 shows interconnections among VoxelPrint components forming the basic workflow used in this study for numerical modelling. The setup defines voxel geometry, material properties, and print parameters required for generating the Abaqus input file.

Using the BrepToVoxel component, the geometry was discretised into a set of three-dimensional cubes – so-called voxels. Voxels represent the three-dimensional equivalent of two-dimensional pixels. Their position is determined by the decomposition of the printing path, where the key parameters

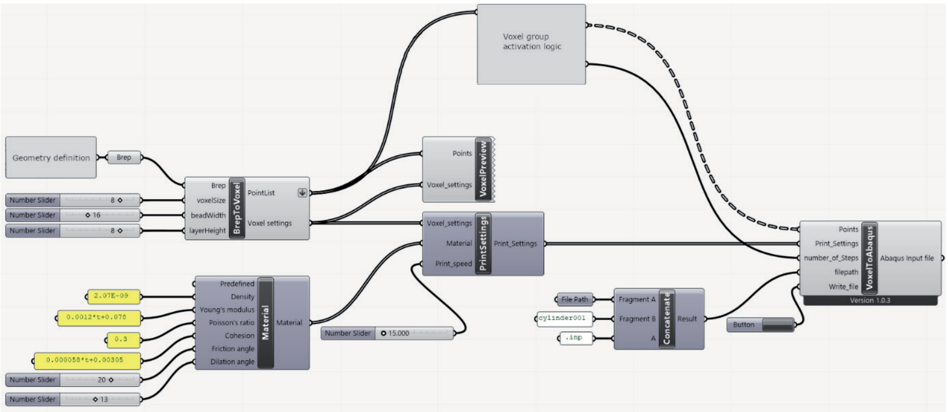

Figure 1: Interconnections among the VoxelPrint components.

are the width of the deposited bead and the voxel size, which defines the level of spatial discretization [12,16].

Two voxel sizes, 8 mm and 4 mm were investigated to evaluate the sensitivity of the numerical results to the degree of spatial discretization. The parameter settings of the BrepToVoxel component for a voxel size of 8 mm are shown in Figure 2.

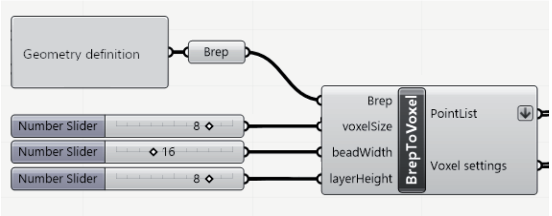

Figure 2: BrepToVoxel component – parameter settings for a voxel size of 8 mm.

The numerical model was based on a time-dependent Mohr–Coulomb failure criterion and linear stress–strain behaviour up to failure. The material used was fresh concrete, with material properties adopted from Wolfs et al. [17].

Time-dependent properties are given by

$$E(t) = 0.0012t + 0.078, \quad (1)$$

$$C(t) = 0.000058t + 0.00305. \quad (2)$$

where E is Young's modulus [MPa] determined at 5% strain, C – cohesion [MPa], t – concrete age [min] [12,17].

The material constants were angle of internal friction φ = 20°, dilation angle ψ = 13°, density ρ = 2070 kg.m^{-3} and Poisson's ratio υ = 0.3 [12,17].

Figure 3 shows the parameter settings of the Material component.

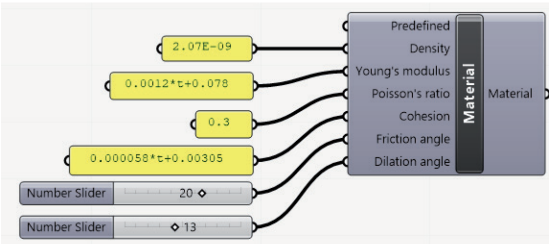

Figure 3: Material component – parameter settings.

The printing speed was set to 15 mm/s in PrintSettings component. After defining the parameters and connecting all required components in VoxelPrint, an input file was generated and imported into Abaqus/CAE. The voxelised geometry was represented by a Part discretised with eight-node solid brick elements (C3D8), with each voxel corresponding to one finite element. Analyses were performed in Abaqus/Standard using a Static, General procedure. In the initial step, all elements were deactivated, and in subsequent steps, element sets were activated stepwise along the toolpath using Model Change (ADD with strain). The self-weight of the material was applied as a gravitational body load, and the base surface of the first layer was fully fixed.

3. Results

The numerical analysis captures the progressive development of plastic deformation and the emergence of the failure mechanism within the printed cylindrical wall. Two main response quantities were evaluated – radial displacements and plastic strains. Radial displacements along the cylinder height were used to describe the global deformation pattern and to monitor the growth of lateral deflection leading to instability, while plastic strain (PE) served to identify the onset and evolution of yielding within the structure.

Figure 4 shows the radial displacement along the predefined evaluation path following the height of the cylinder for both voxel sizes, evaluated at selected activation steps corresponding to different numbers of deposited layers prior to the onset of collapse. In both discretisations, the radial displacement remains negligible near the base, while progressive layer activation leads to increasing displacement amplitudes with similar curve shapes, indicating the development of a flexural instability mode affecting the entire wall height. For the model discretized with 8 mm voxels, the onset of slight swaying of the wall appeared after the deposition of approximately 31 layers, marking the beginning of the instability process. In the finer 4 mm model, the first signs of instability were observed earlier, after about 21 layers, indicating that the onset occurred sooner due to the higher spatial resolution.

In the model with a voxel size of 8 mm, global loss of stability of the wall occurred during the deposition of the 49th layer. At this stage, the previously initiated swaying of the upper layers rapidly intensified, developing into a pronounced buckling mode. Following the onset of elastic buckling, plastic strains started to develop in the region of maximum curvature, indicating the transition from elastic instability to an elastic-plastic post-buckling regime.

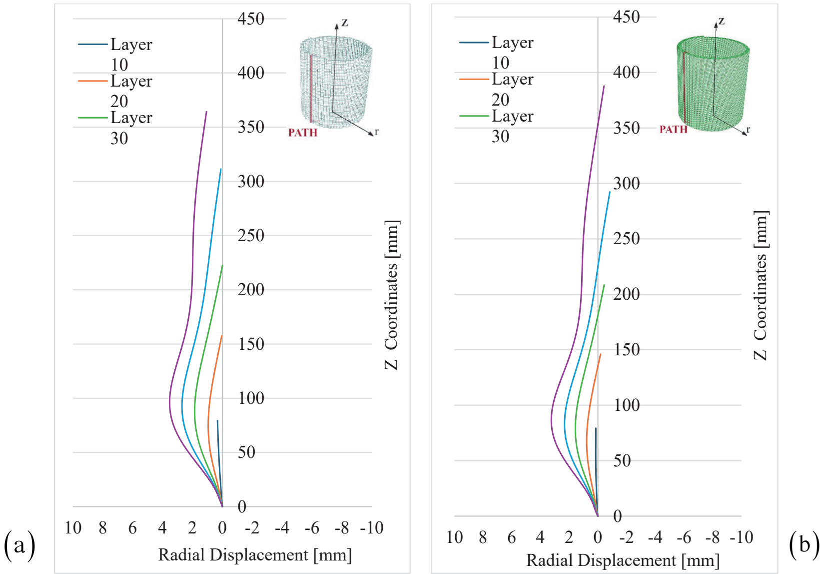

Figure 4: Radial displacement along the cylinder height for models with different voxel sizes: Voxel size 8 mm. (b) Voxel size 4 mm.

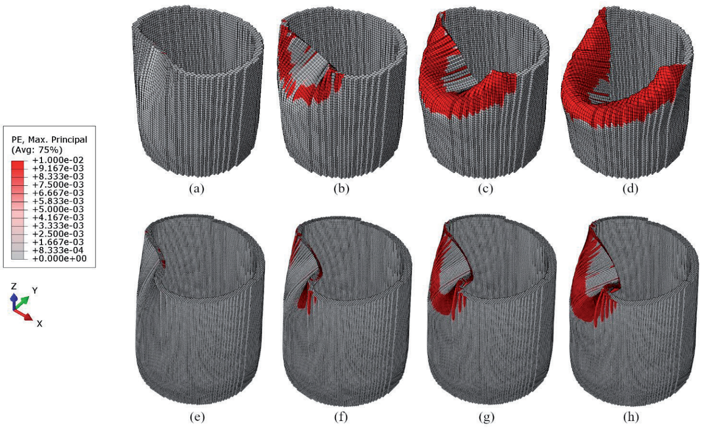

Figure 5: Numerical results of PE, Max. Principal in 3D-printed cylindrical walls for two voxel sizes: (a – d) Voxel size = 8 mm (increments 35, 45, 80, 300). (e – h) Voxel size = 4 mm (increments 30, 35, 40, 47).

The model with a finer voxel size of 4 mm exhibited the same overall behaviour, with the buckling mode initiating in the upper part of the wall during the deposition of the 51st layer and subsequently accompanied by localised plastic deformation. Owing to the higher spatial resolution, the distribution of plastic strain was captured with greater accuracy, revealing more distinct localisation zones but maintaining the same overall instability mechanism and confirming that the predicted buildability limit is only weakly sensitive to the adopted mesh size.

Figure 5 presents the evolution of plastic strain (PE, Max. Principal) in the 3D-printed cylindrical walls for both voxel sizes, illustrating how plastic deformation initiates in the upper part of the wall and progressively localises in the region of maximum curvature as instability develops. The figure shows the failure mechanism, with the colour scale modified for visualization purposes. The results correspond to selected representative increments within the final printing step, captured during the deposition of the last layer at which collapse occurred.

Table 1 summarises the key buildability results for both discretisations.

Table 1: Summary of buildability results for both voxel discretisations.

Voxel size [mm]	Number of fully activated layers before failure	Layer at which failure initiated	Critical build height [mm]	Max. principal plastic strain (PE)
8	48	49	392	0.6828
4	50	51	408	0.4068

4. Conclusions

This study addressed the buildability of an extrusion-printed cylindrical concrete wall at early age by combining the VoxelPrint plug-in in Grasshopper with the Abaqus/Standard solver. The workflow enabled the generation of voxelised geometries, time-dependent material definitions, and stepwise element activation along the printing toolpath, providing a numerically efficient framework for simulating the layer-by-layer printing process under the self-weight. In both discretisations, plastic strains occurred only in the upper layers of the wall, concentrated in the zone of maximum radial displacement, while the lower part of the cylinder remained essentially elastic. The resulting failure mechanism may be regarded as an elastic–plastic buckling of the upper wall segment under self-weight. The finer discretisation predicted a slightly higher critical build height than the coarser one, but the difference was small and the qualitative failure mode was unchanged, indicating only a weak sensitivity of the buildability limit to the adopted element size for the analysed configuration.

Acknowledgments

This work was supported by European Union under the REFRESH–Research Excellence for REgion Sustainability and High-tech Industries project number CZ.10.03.01/00/22_003/0000048 via the Operational Programme Just Transition, the project No. CZ.02.01.01/00/22_008/0004631 Materials and technologies for sustainable development within the Jan Amos Komensky Operational Program; by the Slovak Research and Development Agency under the project APVV-23-0461, and by the Ministry of Education, Research, Development and Youth of the Slovak Republic under the project VEGA No. 1/0342/24.

References

1. ISO/ASTM 52900 (2021). Additive manufacturing – General principles – Fundamentals and vocabulary. International Organization for Standardization. Geneva.
2. De Witte, D (2022). Clay Printing: The Fourth Generation Brickwork. Springer, Germany.
3. Zhao, Q., et al. (2025). Advances and Application Potential in the Research of Silicate Mineral-Based 3D Printing Materials. Progress in Materials Science, 152, 101450.
4. Carter, C. B, Norton, M.G. (2013) Ceramic Materials Science and Engineering, 2nd edition. Springer, New York, 766 p.
5. Romanczuk-Ruszuk, E., et al. (2023). 3D Printing Ceramics—Materials for Direct Extrusion Process. Ceramics, 6, 1, 364–385.
6. Cuevas, D. G., Pugliese, G. (2020) Advanced 3D Printing with Grasshopper: Clay and FDM. 1st edition. Kindle Direct Publishing, 195 p.
7. Li, Z., et al. (2020). Fresh and Hardened Properties of Extrusion-Based 3D-Printed Cementitious Materials: A Review. Sustainability, 12, 14, 5628.
8. Malaeb, Z. et al. (2015). 3D Concrete Printing: Machine and Mix Design. International Journal of Civil Engineering and Technology, 6, 6, 14-22.
9. Wolfs, R. J. M., Suiker, A. S. J. (2019) Structural Failure During Extrusion-Based 3D Printing Processes. The International Journal of Advanced Manufacturing Technology, 104, 565–584.
10. Suiker, A. S. J. (2018). Mechanical Performance of Wall Structures in 3D Printing Processes: Theory, Design Tools and Experiments. International Journal of Mechanical Sciences, 137, 145–170.
11. Khan, S. A., Koç, M. (2022). Numerical Modelling and Simulation for Extrusion-based 3D Concrete Printing: The Underlying Physics, Potential, and Challenges. Results in Materials, 16, 100337.
12. Vantyghem, G., Ooms, T., de Corte, W. (2021) VoxelPrint: A Grasshopper Plug-In For Voxel-Based Numerical Simulation of Concrete Printing. Automation in Construction, 122, 103469.
13. Pierre, M. et al. (2025). Multiphysics Modelling of 3D Concrete Printing: From Material Model to Process Simulation and Optimisation. Additive Manufacturing, 109, 104847.
14. Spangenberg, J., et al. (2021) Numerical Simulation of Multi-Layer 3D Concrete Printing. RILEM Technical Letters, 6, 119-123.
15. Ann, D., Zhang, Y. X., Yang, R. (2024). Numerical Modelling of 3D Concrete Printing: Material Models, Boundary Conditions and Failure Identification. Engineering Structures, 299, 117104.
16. Vantyghem, G., Ooms, T., de Corte, W. (2020). FEM Modelling Techniques for Simulation of 3D Concrete Printing. preprint
17. Wolfs, R. J. M., Bos, F. P., Salet, T. A. M. (2018). Early Age Mechanical Behaviour of 3D Printed Concrete: Numerical Modelling and Experimental Testing. Cement and Concrete Research, 106, 103–116.